

# Effects of Local Reinforcement on Nozzles in Dished Ends

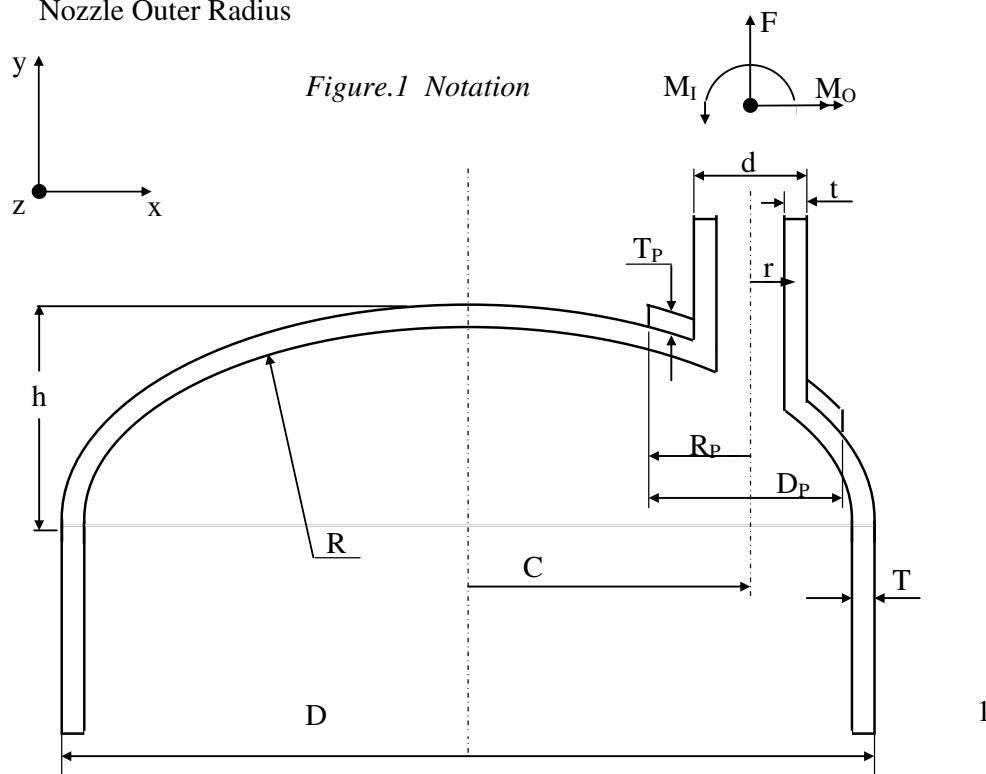
D H Nash and J Hitchen

## Abstract

The results of a parametric design study, to determine the optimum diameter of reinforcing pad for nozzles in the knuckle region of an ellipsoidal pressure vessel head are presented herein. The study utilised a linear elastic finite element model, created using ANSYS finite element analysis software. Nozzle parameters of diameter, offset, and wall thickness were varied to ensure the results obtained were achieved through a thorough analysis. Optimum pad sizes were obtained for thrust, in plane moment and out-of-plane moment nozzle loads. Design curves were produced, allowing maximum permitted applied stress, to be calculated for any nozzle size subject to one of the three loading conditions. Recommendations for allowable offset and treatment of loading combinations are also presented.

## Notation

A	Nozzle Cross-section Area	R	Dished End Mean Radius
C	Nozzle Offset	$R_P$	Reinforcement Pad Radius
d	Nozzle Outer Diameter	$R_V$	Vessel Inner Radius
D	Vessel Outer Diameter	$S_{INT}$	Stress Intensity
$D_P$	Reinforcement Pad Diameter	SCF	Stress Concentration Factor
E	Young's Modulus	t	Nozzle Thickness
F	Axial Thrust	T	Vessel Thickness
FEA	Finite Element Analysis	$T_P$	Reinforcement Pad Thickness
h	Head Height	$\sigma_{ALLOW}$	Allowable Design Stress
I	Second Moment of Area	$\sigma_\theta$	Circumferential Stress
$M_I$	In-Plane Moment	$\sigma_Y$	Yield Stress
$M_O$	Out-of-Plane Moment	X	Function of die-out Distance
r	Nozzle Outer Radius		



## **Introduction**

Cylindrical pressure vessels are often closed with dished ends which are either torispherical or ellipsoidal in shape. High stresses occur in the “knuckle” region of the dished end, due to edge bending effects, caused as the cylinder and head try to deform in different directions. For functional reasons it is often necessary to place a nozzle in the knuckle region, further compounding the complexity of the stress system in this area.

In the European Standard, EN13445 [1] no part of a nozzle is permitted in the outer ten percent of the diameter of a dished end. This constraint prevents nozzles from being placed in over a third of the overall surface area of a dished end – greatly inhibiting pressure vessel design. This rule was put in place since the stress system around a nozzle in the knuckle region is too complicated to be analysed using shell analysis. However the stresses in almost any geometry, can be assessed by the use of a design-by-analysis approach.

Hsieh et al [2], used an FE approach to determine stress levels for knuckle-encroaching nozzles in a torispherical head, subject to various loads. They found that for applied moment and thrust loads, stresses were lowered by maximising the offset of the nozzle into the knuckle region.

Gilmour [3] used FEA to determine the optimum dimensions for reinforcement pads, required for knuckle-encroaching nozzles in an ellipsoidal dished end, subject to internal pressure loading. His body of work concluded that the addition of a reinforcing pad reduces the stress concentration at the nozzle-shell intersection. It was also found that reinforcing pad diameter had a greater effect on the SCF than the reinforcing pad thickness.

The work carried out in the present study, considers the optimum pad diameter required for knuckle encroaching nozzles in a 2:1 ellipsoidal dished end, for nozzle loads of axial thrust, in-plane moment and out of plane moment. ANSYS finite element analysis software was used to build and analyse a suitable model. The pad diameter was the parameter which was optimised, the pad thickness was kept constant throughout the study.

## **Finite Element Modelling**

In order to conduct the investigation, a parametric finite element model was created using ANSYS finite element modeling software. All models were produced using twenty-noded three-dimensional structural solid brick elements, with three translatory degrees of freedom per node (ANSYS element SOLID95).

The model was constructed from a cylindrical vessel attached to a 2:1 ellipsoidal dished end, the vessel wall thickness was constant throughout the structure. The nozzle was modelled as flush with the inside of the vessel and no weld detail was included. The geometric dimensions of the model created and the material properties used are detailed in Appendix A. The nozzle diameter, nozzle thickness and nozzle offset were altered in the study. These parameters were assessed subject to three load conditions; thrust, in-plane moment and out-of-plane moment.

To minimise the size of the model (and computer resources) only a quarter of the dished end was created, though this included a half model of the nozzle due to the significant nozzle offset. The model was discretized into four-sided areas, to allow the use of quadrilateral shaped elements which tend to produce more accurate results, than more irregular shapes. The mesh was graded, with small elements at the nozzle and pad, and larger elements away from the point of interest.

### Parameter Study

The parameter study involved solving the finite element model extensively for; nine nozzle sizes (shown in Appendix A); thrust, in-plane and out-of-plane moment loading; offsets of  $C/R_v = 0.6$  and  $C/R_v = 0.75$ ; as well as numerous iterations in pad size. The model was solved assuming a small displacement linear elastic analysis. The use of unit loads throughout the analysis ensured that yield stress was not approached in the model. For every pass of the finite element model, the parameters involved and the maximum Tresca (Stress Intensity) and Von Mises stress results were recorded in reference [6].

The objective of the parameter study was to develop parametric relations which could be used to determine optimum reinforcing pad diameters. This was achieved by making the reinforcing pad diameter a function of nozzle outer diameter, and then plotting this ratio against the maximum SCF. Graphs were then produced for each nozzle size and load type [6], one such example is shown in Figure 2.

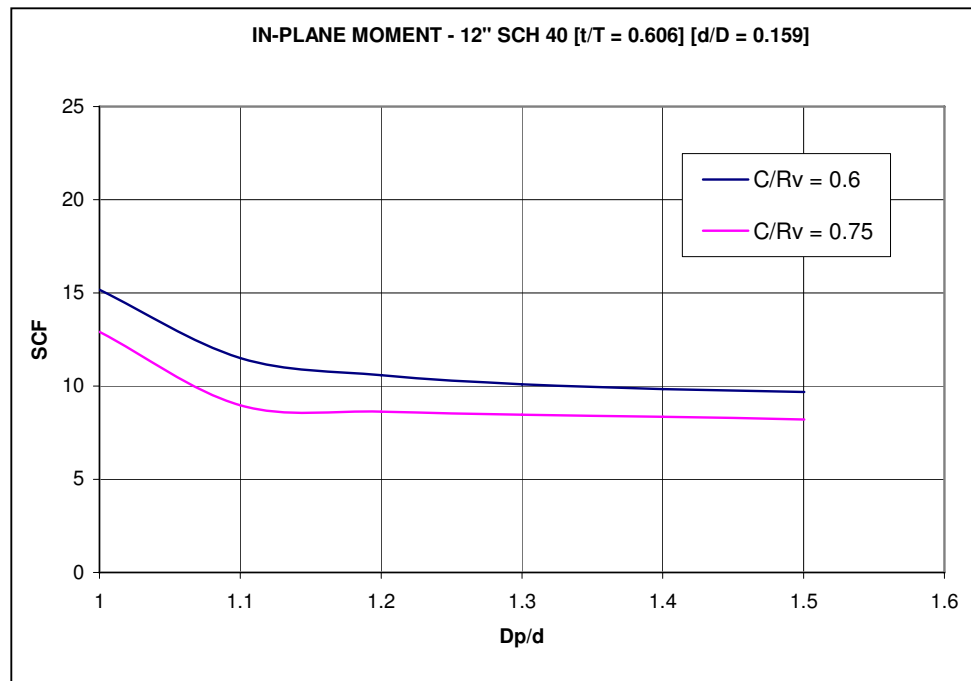


Figure 2. Example of Parameter Study Graph.

SCF values were attained by dividing the recorded maximum Tresca stress by a nominal stress value. The nominal stress values used for the different loading types are shown in Table 1.

Loading Type	Nominal Stress
--------------	----------------

Thrust	$\sigma = \frac{F}{A}$
In-Plane Moment	$\sigma = \frac{M_I d}{2I}$
Out-of-Plane Moment	$\sigma = \frac{M_{Od}}{2I}$

Table 1. Nominal Stress Values.

For all nozzles and loading types analysed, lower SCF occurred at the higher offset. The parameter study showed that for axial thrust loading the maximum stress is very much dependant on the t/T ratio. For thin nozzles (t/T<1) the maximum stress occurred in the nozzle (as illustrated by Figure 3), whilst for thicker nozzles the maximum stress occurred in the vessel. This occurred since the thinner nozzles are flexible and therefore prone to deformation, whilst the thicker nozzles are very stiff and transfer the loading to the vessel, which in turn is forced to deform.

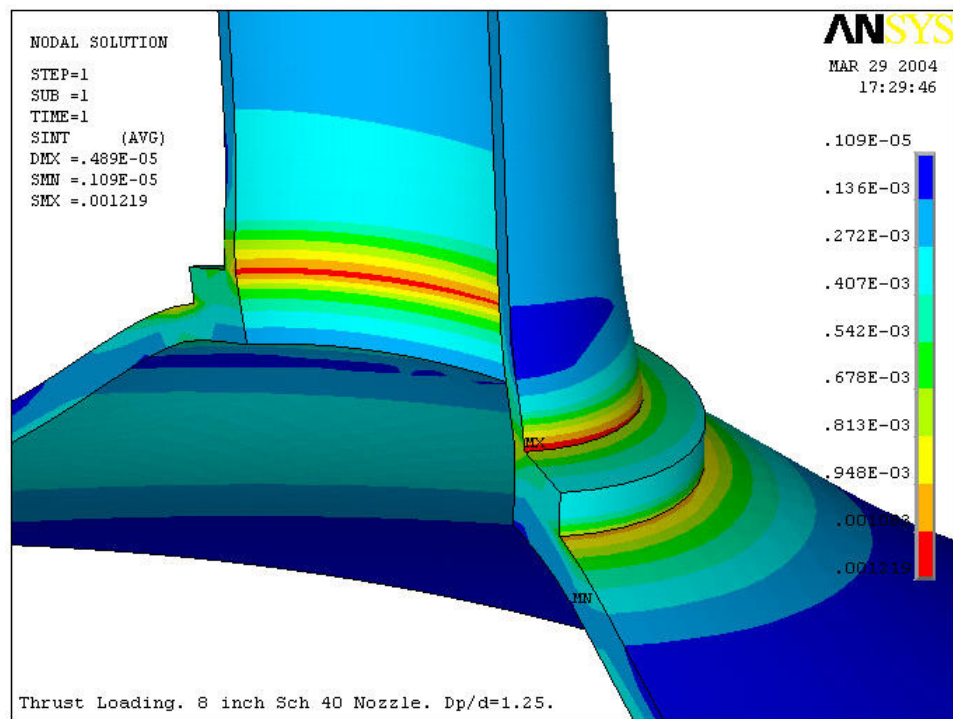


Figure 3. Stress Intensity Contour Plot. 8" Sch 40. Dp/d=1.25. C/Rv=0.6.

For in-plane moment loading, d/D has a significant effect on the magnitude of the SCF. The maximum stress occurred in the nozzle for all but the largest nozzle studied. An example of the stress distribution due to in-plane moment loading is displayed in Figure 4, which shows that raised stresses occur in the knuckle region.

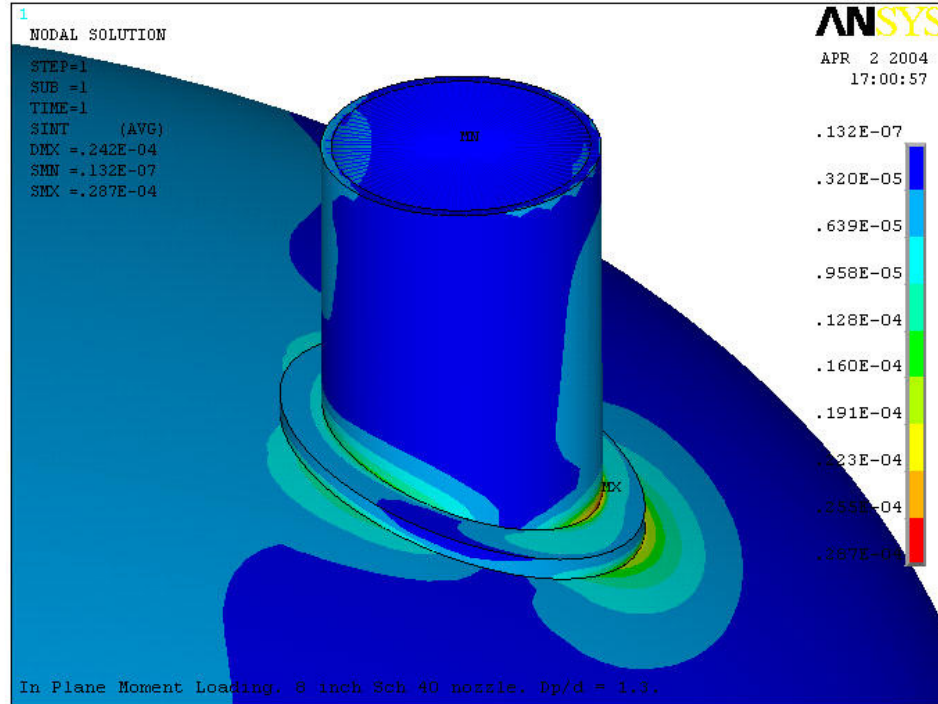


Figure 4. Stress Intensity Contour Plot. 8" Sch 40.  $D_p/d=1.3$ .  $C/R_v=0.6$ .

For out-of-plane moment loading, curves for the two offsets converged on the same value of SCF. Convergence of the two curves occurred at different values of  $D_p/d$  for each nozzle. The value of  $D_p/d$  for convergence to occur was linked to both  $t/T$  and  $d/D$  ratios. As was the case with thrust loading, for thin nozzles the maximum stress concentration occurred in the nozzle, whilst for thick nozzles the maximum stress occurred in the vessel. An example of the stress distribution due to in-plane moment loading is shown in Figure 5.

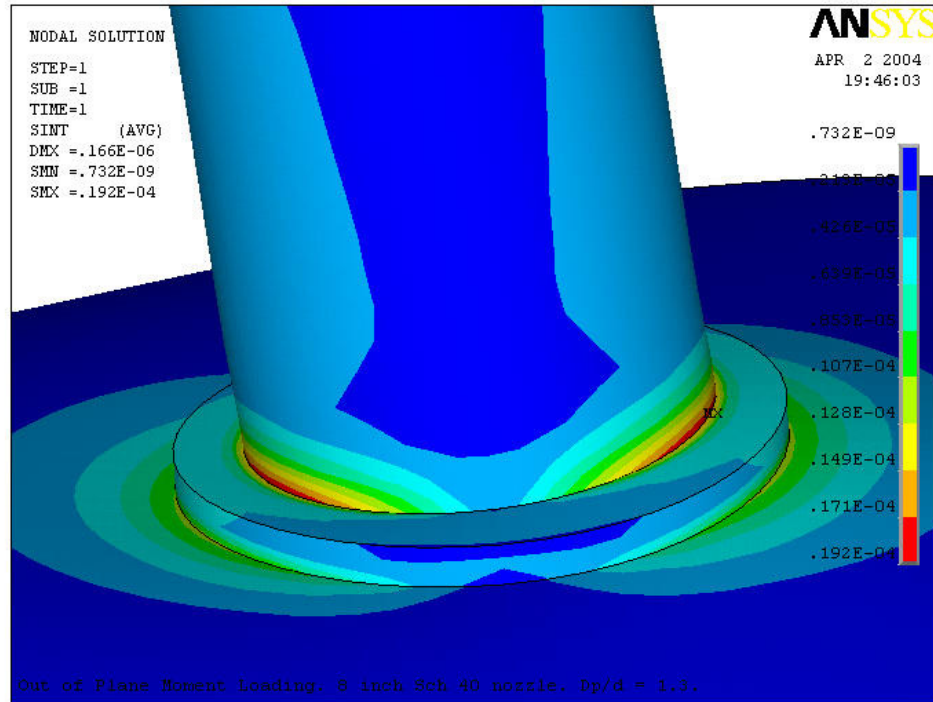


Figure 5. Stress Intensity Contour Plot. 8" Sch 40.  $D_p/d=1.3$ .  $C/R_V=0.6$ .

### Optimum Reinforcing Pad Diameter

The FEA results were examined to determine trends and relationships, from which optimum values of reinforcing pad diameter could be established. Over a specific “die-out” distance from the nozzle, a reinforcing pad will have the effect of lowering stresses. Increased reinforcement beyond the die-out distance will not further reduce the magnitude of stress. Thus reinforcement is required only over the distance where discontinuity stresses are acting. Where possible, optimum values of  $D_p/d$  represented a pad which covered the die-out stress. In cases where this would make the pad size excessive, a smaller  $D_p/d$  ratio was chosen, which had the effect of significantly reducing SCF.

In order to conduct the study effectively, a relationship involving the stress die-out function  $\sqrt{RT}$ , the nozzle radius (r) and the optimum radius of reinforcing pad was established. The relation used was Equation 1, where X indicates a function  $\sqrt{RT}$ .

$$R_p = X \sqrt{RT} + r$$

Shown in Table 2 are the optimized sizes of reinforcing pad for each nozzle radius and each loading type, together with the corresponding value of X.

Type of Loading	X	8" Nozzle r =109.5 mm		12" Nozzle r =161.9 mm		16" Nozzle r =203.2 mm	
		R <sub>p</sub> (mm)	D <sub>p</sub> /d	R <sub>p</sub> (mm)	D <sub>p</sub> /d	R <sub>p</sub> (mm)	D <sub>p</sub> /d
Thrust	0.35	174.6	1.59	227	1.4	268.3	1.32
In-Plane Moment	0.3	165.3	1.51	217.7	1.34	259	1.27
Out-of-Plane Moment	0.3	165.3	1.51	217.7	1.34	259	1.27

Table 2. Optimised Reinforcing Pad

### Design Curves

The stress concentration factors associated with the optimum pad dimensions, were used to calculate the maximum allowable design stress for each type of loading. Since linear elastic FEA had been used, design stress was calculated as below yield with a factor of safety of 1.5.

An alternative way of obtaining design stresses would have been to calculate the limit load of the model by an elastic perfectly plastic FEA, and then stating the maximum permitted design stress as limit-load/1.5. However such a method would allow plasticity to occur in the complex stress field at the dished end knuckle region, which would lead to a point of weakness that may result in the head buckling. Hence the more conservative elastic analysis was used.

Expressions for design stress were created for each type of loading as shown in Table 3. Incorporated in the expressions is a factor of safety of 1.5.

Loading Type	Allowable Design Stress Expression
Thrust	$\frac{\sigma_{\text{ALLOW}}}{\sigma_Y} = \frac{F_{\text{ALLOW}}}{A\sigma_Y} = \frac{2}{3 \text{ SCF}}$
In-Plane Moment	$\frac{\sigma_{\text{ALLOW}}}{\sigma_Y} = \frac{M_{\text{IALLOW}}d}{2I\sigma_Y} = \frac{2}{3 \text{ SCF}}$
Out-of-Plane Moment	$\frac{\sigma_{\text{ALLOW}}}{\sigma_Y} = \frac{M_{\text{OALLOW}}d}{2I\sigma_Y} = \frac{2}{3 \text{ SCF}}$

Table 3. Design Stress

Values of SCF were obtained from the parameter study results [6], for optimised D<sub>p</sub>/d ratios, the equations in Table 3 were then used to obtain values for design stress (normalised by yield stress). These values were then plotted for a range of t/T values to give a spread of points. The lower bound of these points were used to create the design curves shown in Figures 6-8, for thrust, in-plane moment and out-of-plane moment. From these curves, values of allowable loading may be found for any size of nozzle.

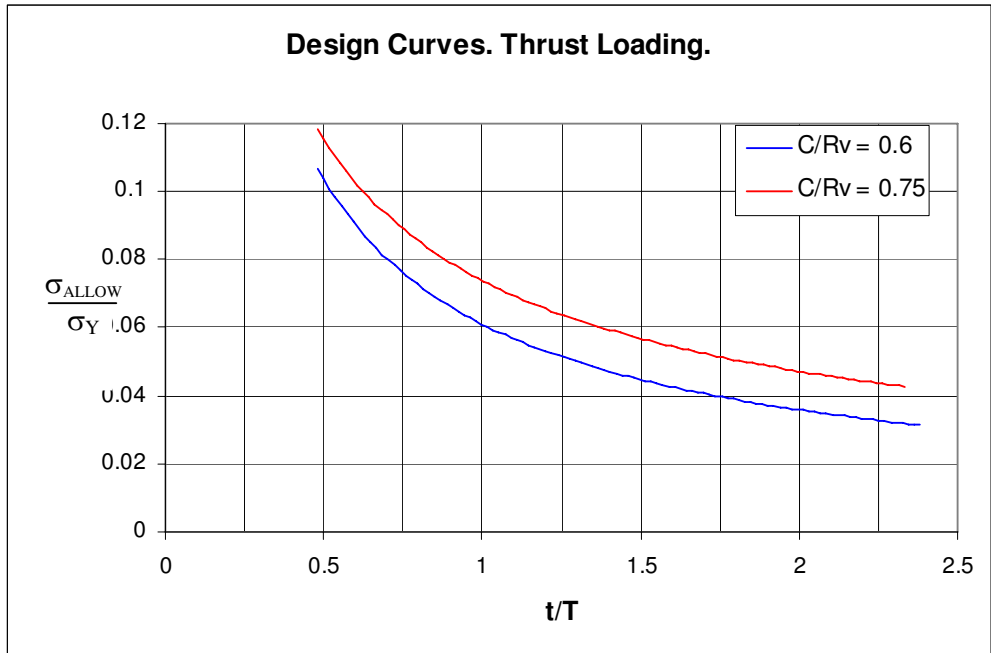


Figure 6. Design Curves for Thrust Loading.

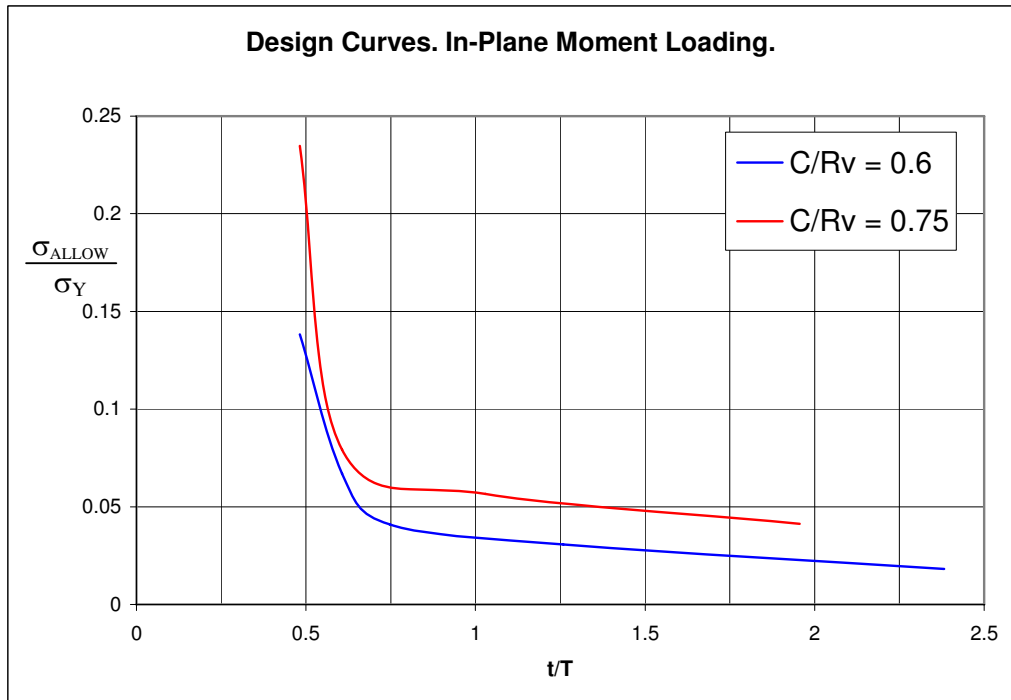


Figure 7. Design Curves for In-Plane Moment Loading.

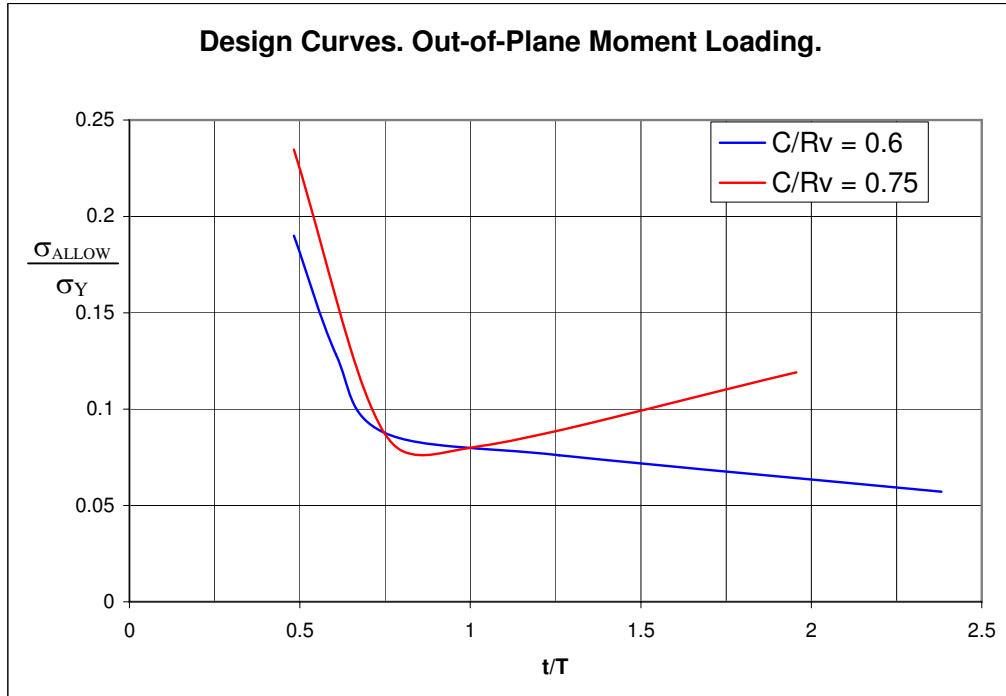


Figure 8. Design Curves for Out-of-Plane Moment Loading.

### Effect of Offset

A generic nozzle size of 8" Sch 40 ( $t/T = 0.482$ ,  $d/D = 0.108$ ) was chosen to demonstrate the effect that offset variation has on SCF. The optimum sizes of pad were used for each of the loading conditions. A range of offsets were considered up to the maximum. Figure 9 shows a graph of the variation of SCF with nozzle offset for the three types of loading considered. For all loading types the SCF was reduced by increasing the nozzle offset, with the lowest stress concentration factors occurring at the highest offsets. Figure 9 indicates that thrust loading had the most significant effect on the model causing the highest values of SCF, followed by in-plane moment loading, with out-of-plane moment loading causing the lowest SCF. The downward trend in SCF for these curves, agrees with the downward trend of the graphs produced by Hsieh, Moffat and Mistry [5], for unreinforced nozzles in a torispherical head with similar offsets. However the gradients in Figure 9 are more shallow than those in [5] which may be due to the different dished end geometries used and effect of the reinforcing pad.

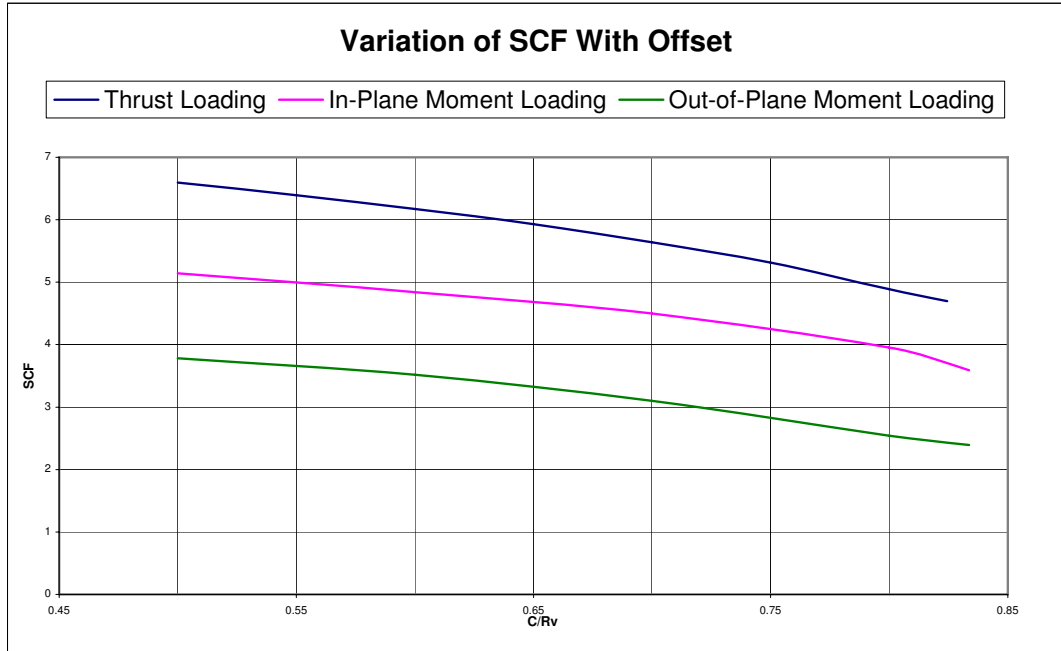


Figure 9. Stress Concentration Factor Variation With Nozzle Offset.

### Combinations of Loading

The effect that combinations of loading have on the stresses in the knuckle region of dished end has not been determined. The maximum stress in the system can occur in either the nozzle or the dished end, depending on the nozzle and load type. Thus a relationship determining how load types would interact, and the effect this would have on the maximum stress would be unfeasibly complicated, and dependant on several parameters.

A brief study into load interaction effects was conducted using a generic nozzle size of 8" Sch 40 ( $t/T = 0.482$ ,  $d/D = 0.108$ ). The optimum size of pad for moment loading was used throughout. The maximum nozzle offset was used, placing the nozzle in the knuckle region. The maximum Tresca stress for thrust, in-plane moment and out of plane moment loading were obtained from running the model in ANSYS. The model was then solved for the loading combinations; thrust and in-plane moment, thrust and out-of-plane moment, in-plane moment and out-of-plane moment, and a combination of all three load types (recorded in [6]). The maximum Tresca stresses for these combinations were compared with the Tresca stresses from the individual loadings. Unit loads were applied for each type of loading, i.e. 1N for thrust and  $1\text{N/mm}^2$  for moment.

All of the maximum Tresca stress results were normalized, by dividing by the maximum Tresca stress for thrust loading. Thus all of the load types were compared to the thrust loading, the results of this process are shown in Table 4.

Applied Loads	$\frac{\sigma}{\sigma_{\text{THRUST}}}$
<b>F</b>	1.0000

$M_I$	0.0154
$M_O$	0.0103
$F + M_I$	0.8755
$F + M_O$	0.8855
$M_I + M_O$	0.0182
$F + M_I + M_O$	0.8755

*Table 4. Load Combinations.*

The ratios in the table are applicable for any value of maximum stress up to yield stress. Inherent in the ratios is the assumption that the loads applied have the same numerical value e.g.  $F = 200N$ ,  $M = 200N/mm^2$ .

Intuitively combining loads should cause an increase in the stress experienced by the system, however from Table 4 this may not be the case. Table 4 indicates that when a moment load and thrust load are applied in combination, the maximum stress in the system is lower than the case for thrust loading alone. Thus indicating that applying a combination of loads might be recommended as a method for lowering stresses. However more investigation would be required to find relationships between the loading types.

## Discussion

The finite element analysis showed that use of a reinforcing pad for a nozzle in the knuckle region of an ellipsoidal dished end was beneficial, since by the introduction of a pad stress concentration factors were reduced for every nozzle and load type considered. However the model used was an idealisation, with the vessel, nozzle and reinforcing pad modelled as a continuous structure with no weld detailing. In reality further stress raising features would be present in a structure due to material imperfections, and manufacturing tolerances.

For the development of the design curves,  $t/T$  was chosen as the parametric relation to be varied, since it gave reasonable trends in the data for all loading types. More accurate design stress values could have been obtained by having separate curves for values of  $d/D$ , however this would lead to design curves only suitable for the specific parametric ratios used in the study.

With an appropriate reinforcing pad in place, the results indicate that nozzles should be allowed in the knuckle region of an ellipsoidal head. EN13445[1] allows nozzles in the vessel head at small offsets, whilst this body of work shows that higher nozzle offset reduces the SCF for the thrust and moment loadings.

## Conclusions

The introduction of a reinforcing pad around a nozzle in the knuckle region of a dished end is worthwhile, since it will cause a reduction in the stresses experienced by the nozzle and vessel. It was shown that for all sizes of nozzle subject to either thrust, in-plane moment or out-of-plane moment loading, a reinforcing pad significantly reduced the SCF compared to the case where no pad was in place

From the parameter study it was found that the further the nozzle was offset from the dished end centre, the further SCF was reduced, this was the case for all three nozzle loads considered in the study; axial thrust, in-plane and out-of-plane moment loading. The offset study showed that for all three loading conditions the lowest SCF occurred

at the maximum offset, where the nozzle and pad were in the knuckle region of the dished end.

Thrust loading was shown to be the most significant of the loading types considered, as the highest stress concentration factors occurred for this type of loading in the majority of nozzle dimensions. The in-plane moment had the second most significant effect in most cases, whilst the out-of-plane moment loading caused the lowest stress concentration factors.

When loading was applied to thick nozzles (relative to the vessel thickness) significantly higher stresses were caused, than was the case for thin nozzles. This occurred due to the thick nozzles being stiff, and therefore less able to deform and subsequently transferring stresses to the vessel, where deformations would be induced.

Optimum values for reinforcing pad dimensions were recommended, that would provide adequate reinforcement for any size of nozzle. For thrust loading the optimum pad radius recommended was a function  $0.35\sqrt{RT}$  larger than the nozzle radius.

For moment loading the optimum pad radius is a function  $0.3\sqrt{RT}$ , larger than the nozzle radius. This function ensured that the stresses were minimised for the range of nozzles studied, for both the in-plane moment and out-of plane moment case.

The design curves have been produced for thrust, in-plane moment and out-of-plane moment which let the maximum allowable applied load be calculated for any size of nozzle, at offsets of  $C/R_v = 0.6$  and  $C/R_v = 0.75$  provided that only one type of loading is applied at a time. These curves act as a guide to ensure that loads applied to nozzles will not cause yield, in any part of the structure.

When a nozzle in the knuckle region of a dished end is subject to a significant thrust loading, the application of a small moment may reduce the maximum stress, thus increasing the amount of thrust loading that may be applied.

## References

- [1] EN 13445, European Unfired Pressure Vessel Standard, CEN, 2002.
- [2] Hsieh, M.F., Moffat, D.G., Mistry, J, Nozzles in the knuckle region of a torispherical head: stress levels and load interaction effects, *ProcIMEchE, Part E, Journal of Process Mechanical Engineering*, 200, **214**, 31-41.
- [3] Gilmour, F, Effects of local reinforcement on pressure vessel nozzles, *BEng(Hons) Thesis*, University of Strathclyde, 2003.
- [4] ANSYS Commands Reference, ANSYS 7.1 Documentation, ANSYS Inc., 2003.
- [5] Leckie, F.A., Penny, R.K., SCF for the Stresses at Nozzle Intersections In Pressure Vessels, *Welding Research Council Bulletin*, 1963, **90**, 19-26.
- [6] Hitchen, J, Effects of local reinforcement on pressure vessel nozzles, *BEng(Hons) Thesis*, University of Strathclyde, 2004.

## Appendix A

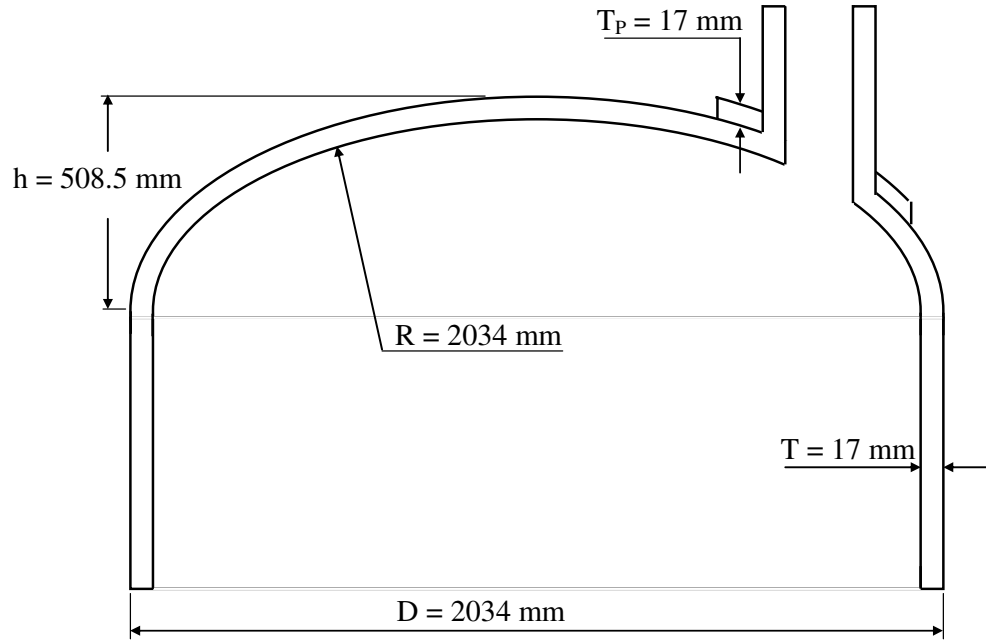


**FIGURE A1. Vessel Dimensions.**

Mean equivalent radius of the dished end:

$$R = \frac{D^2}{4h} = \frac{2034^2}{4 \times 508.5} = 2034 \text{ mm} \quad \text{Hence in this case } R \approx D.$$

Nominal Pipe Size	Outer Diameter (mm)	Wall Thickness (mm)		
		Sch 40	Sch 80	Sch 160
8"	219.1	8.2	12.7	23.0
12"	323.9	10.3	17.5	33.3
16"	406.4	12.7	21.4	40.5

**TABLE A1. Nozzle Sizes (Metric Conversions).**

$$E = 207000 \text{ N/mm}^2$$

$$\sigma_Y = 350 \text{ N/mm}^2$$